

<https://helda.helsinki.fi>

---

## Prolyl oligopeptidase inhibition reduces alpha-synuclein aggregation in a cellular model of multiple system atrophy

Cui, Hengjing

2021

---

Cui , H , Kilpeläinen , T , Zouzoula , L , Auno , S , Trontti , K , Kurvonen , S , Norrbacka , S M , Hovatta , I , Jensen , P H & Myöhänen , T 2021 , ' Prolyl oligopeptidase inhibition reduces alpha-synuclein aggregation in a cellular model of multiple system atrophy ' , Journal of Cellular and Molecular Medicine , vol. 25 , no. 20 , pp. 9634-9646 . <https://doi.org/10.1111/jcmm.16910>

---

<http://hdl.handle.net/10138/339892>  
<https://doi.org/10.1111/jcmm.16910>

---

cc\_by  
publishedVersion

---


*Downloaded from Helda, University of Helsinki institutional repository.*

*This is an electronic reprint of the original article.*

*This reprint may differ from the original in pagination and typographic detail.*

*Please cite the original version.*

# Prolyl oligopeptidase inhibition reduces alpha-synuclein aggregation in a cellular model of multiple system atrophy

Hengjing Cui<sup>1</sup> | Tommi Kilpeläinen<sup>1</sup> | Lydia Zouzoula<sup>1</sup> | Samuli Auno<sup>1</sup> |  
Kalevi Trontti<sup>2,3,4</sup> | Sampo Kurvonen<sup>1</sup> | Susanna Norrbacka<sup>1</sup> | Iiris Hovatta<sup>2,3,4</sup> |  
Poul Henning Jensen<sup>5</sup> | Timo T. Myöhänen<sup>1,6,7</sup> 

<sup>1</sup>Division of Pharmacology and Pharmacotherapy/Drug Research Program, University of Helsinki, Helsinki, Finland

<sup>2</sup>SleepWell Research Program, Faculty of Medicine, University of Helsinki, Helsinki, Finland

<sup>3</sup>Department of Psychology and Logopedics, University of Helsinki, Helsinki, Finland

<sup>4</sup>Neuroscience Center, University of Helsinki, Helsinki, Finland

<sup>5</sup>Department of Biomedicine & DANDRITE, Aarhus University, Aarhus, Denmark

<sup>6</sup>Integrative Physiology and Pharmacology Unit, Institute of Biomedicine, University of Turku, Turku, Finland

<sup>7</sup>School of Pharmacy, University of Eastern Finland, Kuopio, Finland

## Correspondence

Timo T. Myöhänen, Division of Pharmacology and Pharmacotherapy/Drug Research Programme, Viikinkaari 5E (PO Box 56), University of Helsinki, Helsinki 00014, Finland.  
Email: timo.myohanen@helsinki.fi

## Funding information

Academy of Finland, Grant/Award Number: 318327; Jane and Aatos Erkko Foundation and Sigrid Juselius Foundation; Lundbeck Foundation, Grant/Award Number: R248-2016-2518

## Abstract

Multiple system atrophy (MSA) is a fatal neurodegenerative disease where the histopathological hallmark is glial cytoplasmic inclusions in oligodendrocytes, rich of aggregated alpha-synuclein (aSyn). Therefore, therapies targeting aSyn aggregation and toxicity have been studied as a possible disease-modifying therapy for MSA. Our earlier studies show that inhibition of prolyl oligopeptidase (PREP) with KYP-2047 reduces aSyn aggregates in several models. Here, we tested the effects of KYP-2047 on a MSA cellular models, using rat OLN-AS7 and human MO3.13 oligodendrocyte cells. As translocation of p25 $\alpha$  to cell cytosol has been identified as an inducer of aSyn aggregation in MSA models, the cells were transiently transfected with p25 $\alpha$ . Similar to earlier studies, p25 $\alpha$  increased aSyn phosphorylation and aggregation, and caused tubulin retraction and impaired autophagy in OLN-AS7 cells. In both cellular models, p25 $\alpha$  transfection increased significantly aSyn mRNA levels and also increased the levels of inactive protein phosphatase 2A (PP2A). However, aSyn or p25 $\alpha$  did not cause any cellular death in MO3.13 cells, questioning their use as a MSA model. Simultaneous administration of 10  $\mu$ M KYP-2047 improved cell viability, decreased insoluble phosphorylated aSyn and normalized autophagy in OLN-AS7 cells but similar impact was not seen in MO3.13 cells.

## KEYWORDS

alpha-synuclein, KYP-2047, multiple system atrophy, neurodegeneration, prolyl oligopeptidase, synucleinopathies

This is an open access article under the terms of the Creative Commons Attribution License, which permits use, distribution and reproduction in any medium, provided the original work is properly cited.

© 2021 The Authors. *Journal of Cellular and Molecular Medicine* published by Foundation for Cellular and Molecular Medicine and John Wiley & Sons Ltd.

## 1 | INTRODUCTION

Multiple system atrophy (MSA) is a sporadic, adult-onset and progressive neurodegenerative disease with a prevalence of 0.1–3/100,000 persons/year that increases with ageing.<sup>1</sup> Since current therapies are only symptomatic, MSA is a fatal disease with survival duration of 6–9 years after the onset of symptoms. According to the predominant motor disorder, MSA is categorized as MSA-P or MSA-C.<sup>1</sup> Both categories have serious autonomic failure but MSA-P is described mostly by parkinsonism due to the prevailing striatonigral degeneration and MSA-C is characterized by cerebellar ataxia due to olivopontocerebellar atrophy.<sup>1</sup>

The main histopathological hallmark of MSA is the prevalence of glial cytoplasmic inclusions (GCI) in oligodendrocytes.<sup>2</sup> In 1998, Wakabayashi et al.<sup>3</sup> detected that  $\alpha$ -synuclein (aSyn) is the main component of GCI, categorizing MSA to the synucleinopathies with Parkinson's disease (PD) and dementia with Lewy bodies (DLB). Unlike in PD and dementia with Lewy bodies, where aSyn is accumulated mostly in neurons, in MSA aSyn is accumulated in the cytoplasm of oligodendroglial cells.<sup>3</sup> aSyn in GCI is mostly present in a fibrillary oligomeric form<sup>4</sup> and as serine 129 phosphorylated (pS129 aSyn) that is considered to destabilize aSyn and elevate its aggregation.<sup>5</sup> aSyn oligomerization has been shown to cause loss-of-function toxicity, for example in synaptic vesicle regulation, and damage several cellular organelles, including endoplasmic reticulum, mitochondria and protein degradation pathways (for review see<sup>6</sup>). Animal models of MSA have shown that aSyn overexpression in oligodendrocytes causes cellular death, leading to demyelination, neuronal damages and premature death,<sup>7,8</sup> suggesting the involvement of aSyn in the pathophysiology of MSA.

It has been under debate if aSyn in GCI is exogenous and transferred from neurons by cell-to-cell transfer since only low amounts of aSyn mRNA have been measured in healthy and MSA patient-derived oligodendrocytes.<sup>9</sup> However, recent studies suggest that endogenous aSyn in oligodendrocytes is critical for aSyn aggregation in MSA after the exogenous aSyn has triggered the process.<sup>10</sup> Another important factor contributing to aSyn aggregation in MSA is p25 $\alpha$ /TPPP protein (tubulin polymerization-promoting protein; p25 $\alpha$ ). p25 $\alpha$  is a protein promoting tubulin assembly and maintaining myelin sheath<sup>11</sup> but in MSA it relocates from myelin sheaths and accumulates to oligodendroglial soma.<sup>12</sup> This redistribution is associated with demyelination of axons, and subsequently, phosphorylation and aggregation of aSyn, leading to the abovementioned aggregation process.

Compounds having an effect on aSyn aggregation or degradation, such as anle138b<sup>13</sup> or enhancement of aSyn degradation by autophagy activation,<sup>14</sup> respectively, have shown beneficial effects on experimental MSA models. Therefore, targeting aSyn could be a potential disease-modifying therapy for MSA. In our previous studies, we have shown that a serine protease, prolyl oligopeptidase (PREP), increases aSyn oligomerization via direct protein-protein interaction<sup>15,16</sup> and negatively regulates autophagy.<sup>17</sup> Importantly, small-molecular PREP inhibitors can interfere with this interaction,

leading to decreased aSyn aggregation,<sup>15,18,19</sup> and PREP inhibition or deletion also stimulates autophagy and increases the degradation of aSyn oligomers<sup>16–18</sup> and fibrils.<sup>20</sup> In aSyn-based *in vivo* PD model, PREP inhibition has shown disease-modifying impact by restoring an aSyn virus vector-induced behavioural deficit.<sup>21</sup> Therefore, we tested if PREP inhibition has a beneficial effect on aSyn accumulation and toxicity in a cellular model of MSA.

## 2 | MATERIALS AND METHODS

### 2.1 | Reagents

Reagents were purchased from Sigma-Aldrich (St Louis, MO) if not otherwise specified. Ethanol was purchased from Altia (Helsinki, Finland). The PREP inhibitor, KYP-2047 (4-phenylbutanoyl-l-prolyl-2(S)-cyanopyrrolidine), was synthesized by us as described earlier.<sup>22</sup>

### 2.2 | Cell cultures

#### 2.2.1 | OLN-AS7 cell culture

OLN-AS7 cells<sup>23</sup> expressing human aSyn were used in this study. OLN-AS7 originate from immortalized rat oligodendrocyte OLN-93 cell culture that are transfected with a pcDNA3.1 zeo(-) aSyn vector (see<sup>23</sup> for more detailed description). OLN-AS7 cells were maintained at +37°C under 5% CO<sub>2</sub> and grown in full Eagle's medium (DMEM; #D6429) with an additional 10% (v/v) foetal bovine serum (FBS; #16000-044, Thermo Fisher Scientific), 1% (v/v) penicillin-streptomycin solution (#15140122, Thermo Fisher Scientific) and 100  $\mu$ g/ml zeocin (R25005, Thermo Fisher Scientific). For experiments, cells were seeded without zeocin 24 h before treatment. Cells were used for experiments in passages 3–15.

#### 2.2.2 | MO3.13 cell culture

The human oligodendrocyte cell line, MO3.13 (Cedarlane), was obtained from tebu-bio (Roskilde, Denmark), and grown in high glucose Dulbecco's modified Eagle's medium (DMEM) (DMEM-Glutamax; #31966021, Thermo Fisher Scientific) with 10% foetal bovine serum (FBS; #16000-044, Thermo Fisher Scientific) and 1% (v/v) penicillin-streptomycin solution (#15140122, Thermo Fisher Scientific) in a humidified incubator with 5% CO<sub>2</sub> at 37°C. Prior to treatment, cells were seeded in 6-well plates with 4  $\times$  10<sup>5</sup> cells/well density and incubated for 24 h. Cells were used for experiments in passages 3–15.

### 2.3 | Cell treatments

p25 $\alpha$  plasmid transfections in OLN-AS7 cells were done using Lipofectamine 3000 (L3000015; Thermo Fisher Scientific)

according to the manufacturer's instructions 24 h prior to the treatments. Production of pcDNA3.1 zeo(-) plasmid expressing human p25 $\alpha$  is presented in.<sup>24</sup> For MO3.13 cells, p25 $\alpha$  plasmid transfection was performed similar to OLN-AS7 cells, and for aSyn transfection, AAV1-EF1a-V5-synuclein (Addgene #60057; Dr. Brandon Harvey, Intramural Research Program, National Institute on Drug Abuse, Baltimore, MD). aSyn plasmid construction was described in.<sup>17</sup> pAAV-EF1a control vector with 50 bp insert was created as described in.<sup>25</sup> aSyn plasmid concentration was kept similar when transfected with empty plasmid or in combination with p25 $\alpha$  to avoid changes in protein expression, and empty plasmid was used also with p25 $\alpha$  transfection. For PREP inhibitor experiments, KYP-2047 was diluted to cell culture medium from 100 mM stock in 100% DMSO to 1 and 10  $\mu$ M, and corresponding concentration of DMSO was used as a vehicle control.

## 2.4 | PREP enzyme activity assay

For the PREP activity assay, fluorometric assay based on Suc-Gly-Pro-aminomethylcoumarin (AMC) substrate was used as in Myöhänen et al. (2012).<sup>26</sup> Briefly, cells were plated to 6-wellplate with density of 400,000 cells/well, transfected with p25 $\alpha$  and after 24 h, lysed with a lysis buffer. PREP activity was measured from supernatants, and released AMC was correlated on total protein amounts measured by using bicinchoninic acid method (BCA; Pierce BCA Protein Assay Kit, #23225, Thermo Fisher Scientific). All activity measurements were made in triplicate with 2 biological repeats.

## 2.5 | Cell viability assay

OLN-AS7 and MO3.13 cells were plated with the density of 10,000 cell/well in 96-well plate and the next day transfected by p25 $\alpha$  (OLN-AS7) or with p25 $\alpha$  and aSyn (MO3.13). 24 h after transfection, the cells were incubated for 48 h in the presence of 1  $\mu$ M or 10  $\mu$ M

KYP-2047 or DMSO vehicle (0.01% DMSO; 150  $\mu$ l/well). LDH release assay was performed as previously described.<sup>26</sup>

## 2.6 | Immunocytochemistry

Immunocytochemistry (ICC) was used to detect changes in total aSyn, pS129 aSyn and tubulin retraction after p25 $\alpha$  transfection and PREP inhibition. Briefly, OLN-AS7 cells were plated over glass coverslips in a 12-well plate with a density of 60,000 cells/well and allowed to attach overnight. 24 h after p25 $\alpha$  transfection, cells were treated with 10  $\mu$ M KYP-2047 for 48 h and finally fixed with 4% paraformaldehyde for staining. 10% normal goat serum (S-1000, Vector Laboratories) was used for blocking for 30 min and thereafter cells were incubated with primary antibodies against aSyn, pS129 aSyn,  $\alpha$ -tubulin or p25 $\alpha$  overnight at +4°C (details in Table 1). After washes, the following secondary antibodies were used to incubate cells 2 h in room temperature: for sheep aSyn, anti-sheep Alexa Fluor488 (1:400; ab150177, Abcam; RRID: AB\_2801320); for mouse pS129 aSyn, anti-mouse Alexa Fluor488 (1:800; ab150113, Abcam; RRID: AB\_2576208); for rabbit p25 $\alpha$ , anti-rabbit Alexa Fluor 568 (1:800; ab175471, Abcam; RRID: AB\_2576207).  $\alpha$ -tubulin antibody was conjugated with Alexa Fluor 488, and no secondary antibody incubation was used. Cells were mounted with Vectashield containing DAPI to stain nuclei (H-1200, Vector Laboratories; RRID: AB\_2336790). Imaging was performed using Leica TCS SP5 confocal microscope (Leica Microsystems). In tubulin retraction analysis, images were converted to 8-bit grayscale format, and the area of tubulin network in p25 $\alpha$  transfected cells was analysed by ImageJ (version 1.51; National Institute of Health; RRID:SCR\_002285) with a protocol described in.<sup>23</sup> For publication purposes, the images were converted from grayscale to RGB colour and recoloured with corresponding colours, and minor modifications to brightness and contrast were made. All modifications to brightness and contrast were done similarly to each image, and they were analysed prior to modifications.

TABLE 1 Details of antibodies used

Antigen	Species	Manufacturer	Product #/RRID	Dilution
aSyn (ICC and WB)	Sheep	Abcam	ab6162/AB_2192805	1:1000
pS129 aSyn (ICC)	Mouse	Abcam	ab184674/AB_2819037	1:400
pS129 aSyn (WB)	Rabbit	Abcam	ab51253/AB_869973	1:500
p25 $\alpha$ (ICC)	Rabbit	Abcam	ab92305/AB_2050408	1:1000
$\alpha$ -tubulin (ICC)	Mouse	Abcam	ab195887	1:200
PP2AC( $\alpha$ + $\beta$ ); Clone Y119	Rabbit	Abcam	ab32141/RRID:AB_2169649	1:2000
PP2A phospho-Tyr307	Rabbit	Thermo Fisher	PA5-36874/RRID:AB_255379	1:500
LC3B (WB)	Rabbit	Sigma	L7543/AB_796155	1:1000
SQSTM1/p62 (WB)	Mouse	Abcam	ab56416/AB_945626	1:5000
$\beta$ -actin (WB)	Rabbit	Abcam	ab8227/AB_2305186	1:2000
Vinculin (WB)	Rabbit	Abcam	ab129002/AB_11144129	1:10000

Abbreviations: ICC, immunocytochemistry; WB, Western blot.

## 2.7 | Western blot

For Western blot (WB) assays, 200,000 cells were seeded in 6-well plates, transfected with p25 $\alpha$  and treated with 10  $\mu$ M KYP-2047 for 24 or 48 h. Thereafter, the cells were lysed in ice-cold RIPA buffer supplemented with Halt Phosphatase (#87786, Thermo Fisher Scientific) and Protease Inhibitor cocktails (#78430, Thermo Fisher Scientific), sonicated with ultrasonicator and then centrifuged at 14,000 g for 60 min.<sup>17,26</sup> Supernatant was collected as the soluble fraction, and the pellet was dissolved in SDS-containing Laemmli buffer as an SDS-soluble and insoluble fraction.<sup>17,26</sup> Protein concentration was measured from soluble fraction by BCA. 30  $\mu$ g of sample was loaded to 12% stain-free Mini-Protean TGX gels (#4568044, Bio-Rad) for SDS-PAGE. Gels were transferred by Trans-Blot Turbo Transfer System (#1704150, Bio-Rad) onto Trans-Blot Turbo Midi PVDF (#1704157, Bio-Rad) membrane. For insoluble fraction, total protein amount was visualized from stain-free gel by using the ChemiDoc XRS+ (Bio-Rad). Thereafter, the membranes for aSyn and pS129 aSyn immunoblotting were incubated 30 min in 4% paraformaldehyde for fixing. The membranes were blocked with 5% skim milk and incubated in primary antibodies (Table 1) at +4°C overnight. The following HRP-conjugated secondary antibodies were used: goat anti-rabbit (1:2000; #31463; Thermo Fisher Scientific) for pS129 aSyn, vinculin,  $\beta$ -actin and LC3B; donkey anti-sheep HRP (1:2000, ab6900, Abcam; RRID:AB\_955452) for total aSyn; goat anti-mouse HRP (1:5000; #31430; Thermo Fisher Scientific; RRID:AB\_228307) for p62. The images were captured using the ChemiDoc XRS+ (Bio-Rad).

To verify that bands are in the linear range of detection, increasing exposure time and automatic detection of saturated pixels in ImageLab software (version 6.01, Bio-Rad) was used. For analysis, images were converted to 8-bit grayscale format, and the optical densities (OD) of the bands were measured by ImageJ (histogram area analysis). The OD obtained from each band was normalized against the corresponding  $\beta$ -actin (OLN-AS7 cells) or vinculin band (MO3.13 cells), as in our earlier studies.<sup>16,25</sup> All immunoblotting analyses were done with 3–4 technical replicates of each treatment per membrane and with 2–3 biological replicates (at least 3 different WB assays). Full blot images are presented in Supplementary files.

## 2.8 | Quantitative real-time PCR

250 ng of DNase I (Thermo Scientific)-treated total RNA was converted to cDNA with iScript select cDNA synthesis kit (Bio-Rad Laboratories) and amplified with 250 nM of primers in CFX384 Real-Time PCR cycler using IQ SYBR Green Supermix (Bio-Rad Laboratories). Following primers were used for aSyn (*SncA*): forward, AGGACTTCAAAGGCCAAGG; reverse, TCCTCCAACATTGTCACTTGC.<sup>26</sup> Expression levels were normalized to *Actb* (MO3.13 cells: forward GATTCCTATGTGGGCGACGA, reverse ATAGCACAGCCTGGATAGCA, OLN-AS7 cells: forward, ACCCTAAGGCCAACCGTGAA; reverse, TGCTCGAAGTCTAGGGC AAC). Each reaction was run in triplicate, and relative expression

level was calculated using a standard curve (7.15, 10.0, 5.0, 2.0, 1.0, 0.5 and 0.25 ng of cDNA) with CFX Manager (Bio-Rad Laboratories).

## 2.9 | Statistical analyses

All experiments were done at least in triplicate, and samples were not used to re-analyse the same protein. Data are expressed as mean values  $\pm$  standard error of the mean (mean  $\pm$  SEM), and negative control average was set as 100% on each assay to reduce variability between repeats. Error bars in the figures represent SEM if not otherwise stated in the figure legend. Differences between two groups were analysed using two-tailed unpaired Student's *t*-test. For more than 2 groups, 1-way analysis of variance (ANOVA) was followed by Tukey's post hoc comparison if ANOVA assay gave statistical significance ( $p < 0.05$ ). In all cases,  $p < 0.05$  were considered to be significant. Statistical analysis was performed using PRISM GraphPad statistical software (version 6.07, GraphPad Software, Inc.).

## 3 | RESULTS

### 3.1 | PREP inhibition reduces p25 $\alpha$ induced cell death and tubulin retraction in OLN-AS7 cells

Transfection of rat oligodendrocyte cell line stably overexpressing aSyn (OLN-AS7 cells) with p25 $\alpha$  caused a 11% increase in the PREP activity compared to empty Lipofectamine (LFC) transfection (Figure 1A;  $t = 3.338$ ,  $p = 0.0289$ , Student's *t*-test). p25 $\alpha$  transfection also induced cellular death in the LDH cell viability assay 48 h after transfection (Figure 1B; 24% increase compared to LFC control;  $F_{5,35} = 29.32$ ,  $p < 0.001$ , 1-way ANOVA with Tukey's post-test) but when OLN-AS7 cells were treated simultaneously with 10  $\mu$ M KYP-2047, cell survival increased significantly (Figure 1B;  $F_{5,35} = 29.32$ ,  $p < 0.001$ , 1-way ANOVA with Tukey's post-test). Based on cell viability studies, 10  $\mu$ M KYP-2047 was selected for further assays.

Translocation of p25 $\alpha$  to the cytosol leads to loss of its normal function in myelination and this causes microtubule retraction contributing to cellular toxicity.<sup>10,23</sup> Similarly to previous studies, our ICC assay showed that transfected p25 $\alpha$  caused significant decrease in the tubulin area in 48 h compared to LFC control or 10  $\mu$ M KYP-2047 (Figure 1C-F;  $F_{3,73} = 1.358$ ,  $p < 0.05$ , 1-way ANOVA with Tukey's post-test). When p25 $\alpha$  transfection was combined with 10  $\mu$ M KYP-2047, the tubulin retraction was not significant compared to LFC but also not significantly different from p25 $\alpha$ +vehicle (Figure 1C).

### 3.2 | PREP inhibition reduces insoluble total and phosphorylated aSyn in OLN-AS7 cells

An earlier study with OLN-AS7 cells showed that aSyn phosphorylation contributes to microtubule retraction and aSyn toxicity.<sup>23</sup> PREP

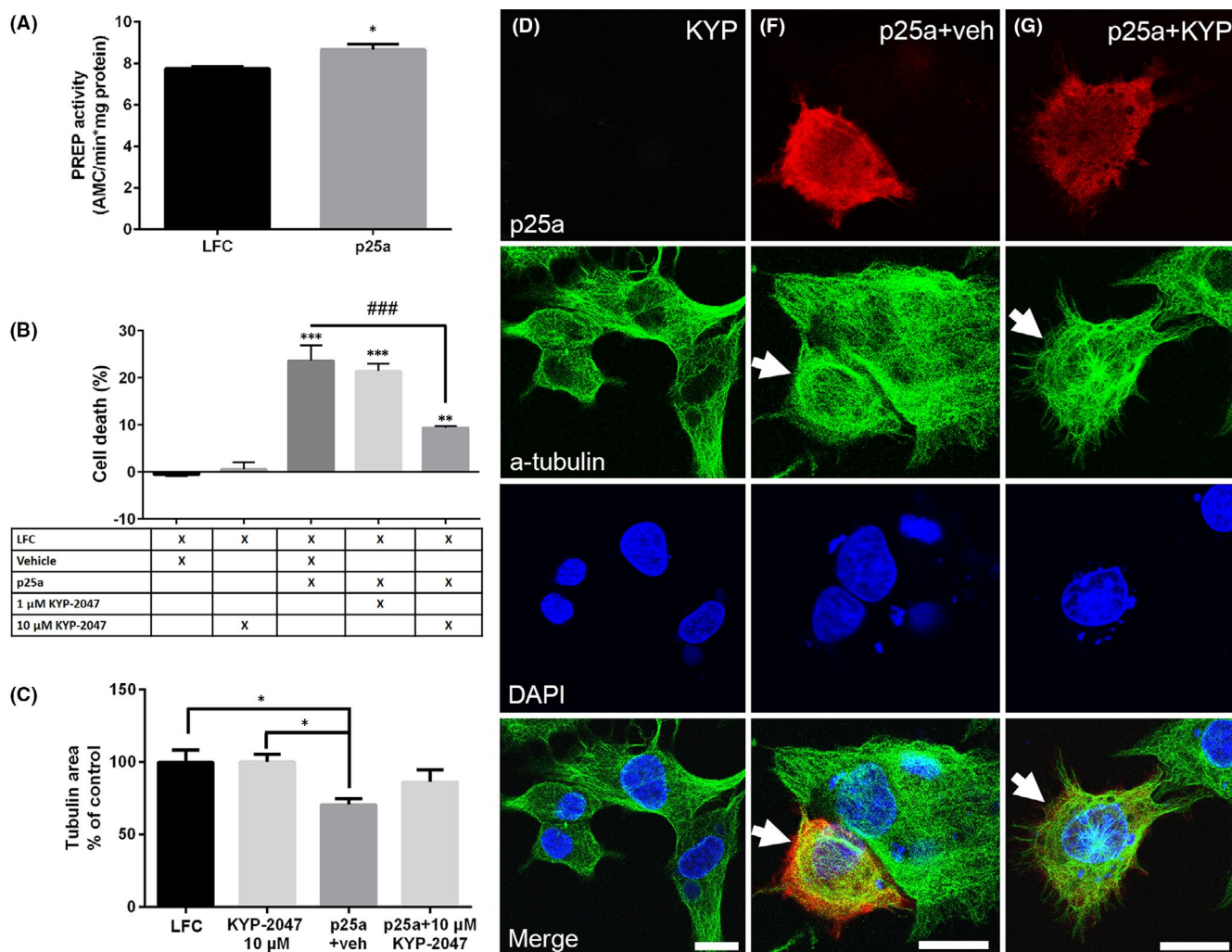


**FIGURE 1** PREP activity increases after p25 $\alpha$  transfection and 10  $\mu$ M KYP-2047 attenuates p25 $\alpha$  toxicity. Transfection of OLN-AS7 cells with p25 $\alpha$  (p25a) caused small but significant increase in PREP activity compared to Lipofectamine control (LFC) (A). p25 $\alpha$  transfection for 48 h also caused significant increase in cell death in the LDH assay compared to LFC control. However, 48 h PREP inhibition with 10  $\mu$ M KYP-2047 after p25 $\alpha$  significantly reduced cellular death compared to p25 $\alpha$ +vehicle (veh; 0.01% DMSO) (B). p25 $\alpha$  transfection with vehicle treatment caused significant tubulin retraction compared to LFC or 10  $\mu$ M KYP-2047 alone while similar impact was not seen between LFC and p25 $\alpha$ +10  $\mu$ M KYP-2047 (C). Representative immunofluorescence pictures showing the effect of p25 $\alpha$  transfection (red) on  $\alpha$ -tubulin (a-tubulin) network (green). 48 h treatment with 10  $\mu$ M KYP-2047 without p25 $\alpha$  transfection had no effect on tubulin (D). p25 $\alpha$  transfection and 48h vehicle treatment led to tubulin retraction (E) but the effect of p25 $\alpha$  was reduced in cells treated for 48 h with 10  $\mu$ M KYP-2047 (F). Number of analysed cell/group in panel C is 30 (LFC); 25 (10  $\mu$ M KYP-2047); 27 (p25a+veh); 24 (p25a+10  $\mu$ M KYP-2047). DAPI was used as a nuclear marker, scale bar is 5  $\mu$ M. Data are presented as mean  $\pm$  SEM. \*,  $p < 0.05$ , Student's *t*-test (A). \*,  $p < 0.05$ ; \*\*\*,  $p < 0.001$ , 1-way ANOVA with Tukey's post hoc test (B-C)

inhibition has reduced the number of aSyn oligomeric particles and particularly insoluble aggregates in our earlier studies,<sup>17,21,26</sup> and therefore, we characterized if KYP-2047 has an impact on aSyn phosphorylation and aggregation in OLN-AS7 cells. We first tested 24 h p25 $\alpha$  transfection but the WB analysis revealed the increase in aSyn and pS129 aSyn levels particularly in SDS fraction were mild (Figure S1). p25 $\alpha$  toxicity has been shown to be the most evident at 48 h after p25 $\alpha$  transfection in OLN-AS7 cells,<sup>23</sup> and therefore, we selected this time-point for further studies. ICC showed that cells transfected with p25 $\alpha$  had increased cytosolic aSyn immunoreactivity (Figure 2A). Interestingly, in p25 $\alpha$  expressing cells, aSyn immunoreactivity was both diffuse and puncta-like while in non-transfected

cells the staining pattern showed mostly puncta-like structures (Figure 2A-B). After transfection, 48 h treatment with KYP-2047 reduced aSyn immunoreactivity in p25 $\alpha$ -positive cells but the puncta-like staining remained in non-transfected cells (Figure 2B). pS129 aSyn showed nuclear expression in OLN-AS7 but in p25 $\alpha$  transfected cells, more intense immunostaining was detected also in the cytosol (Figure 2C). 48 h KYP-2047 incubation reduced cytosolic pS129 aSyn signal in p25 $\alpha$  transfected cells (Figure 2D).

After ICC, we confirmed the changes in protein levels in the soluble fraction and the SDS fraction by WB. WB analysis revealed that at the 48 h time-point total and pS129 aSyn were significantly elevated in the soluble fraction of p25 $\alpha$  transfected cells (Figure 3A-B; total

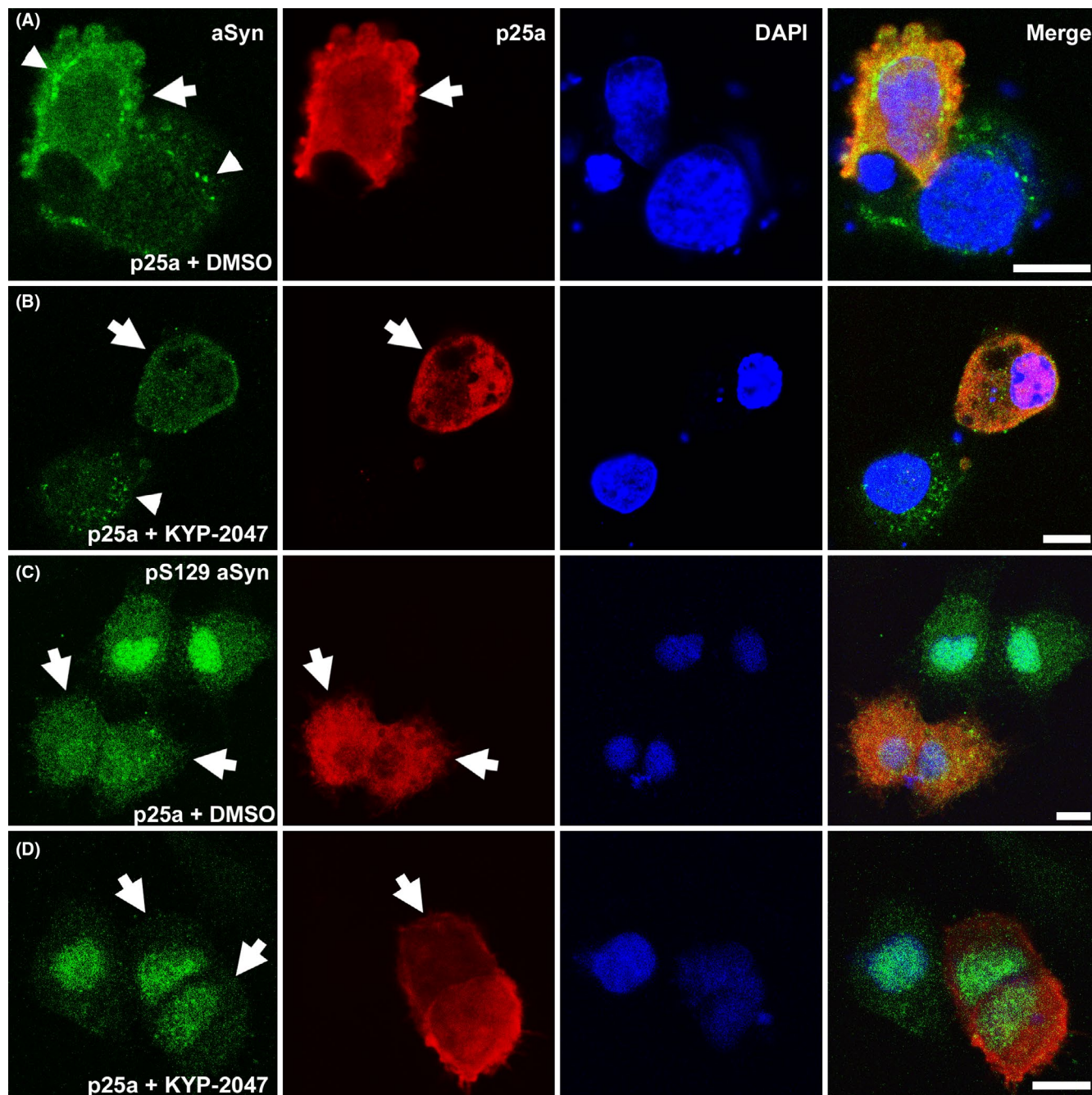


**FIGURE 2** KYP-2047 reduces cytosolic immunoreactivity in p25 $\alpha$ -transfected cells. In cells treated for 48 h with vehicle after p25 $\alpha$  transfection (p25 $\alpha$ +DMSO), p25 $\alpha$  expressing cells (red; white arrow) showed intense cytosolic total aSyn immunostaining (A; green). When cells were incubated for 48 h with 10  $\mu$ M KYP-2047, cytosolic aSyn signal was lowered (B; p25 $\alpha$ +KYP-2047). OLN-AS7 cells expressed aSyn puncta (white arrowheads) that were present both in p25 $\alpha$  transfected and non-transfected cells (cells without p25 $\alpha$  expression (red colour)), and KYP-2047 treatment seemed not to remove them from the cytosol (A-B). Serine 129 phosphorylated aSyn (pS129 aSyn) showed strong nuclear staining but in p25 $\alpha$ -positive cells that were treated with DMSO for 48 h, the staining was also intense in the cytosol (C). 10  $\mu$ M KYP-2047 reduced cytosolic signal of pS129 aSyn (D). DAPI was used as a nuclear marker, scale bar is 5  $\mu$ m

aSyn,  $F_{2,15} = 19.45$ ,  $p < 0.001$  LFC vs. p25 $\alpha$ +vehicle,  $p < 0.05$  LFC vs. p25 $\alpha$ +KYP-2047; pS129 aSyn,  $F_{2,15} = 7.25$ ,  $p < 0.01$  LFC vs. p25 $\alpha$ +vehicle,  $p < 0.05$  p25 $\alpha$ +KYP-2047, 1-way ANOVA with Tukey's post hoc test). KYP-2047 decreased total aSyn levels compared to vehicle treatment but not the pS129 aSyn levels (Figure 3A-B;  $p < 0.05$ , p25 $\alpha$ +vehicle vs. p25 $\alpha$ +KYP-2047, 1-way ANOVA with Tukey's post-test).

Both analysed aSyn forms were also increased in SDS fraction in p25 $\alpha$  transfected groups (Figure 3A-D; total aSyn,  $F_{2,21} = 14.51$ ,  $p < 0.001$  LFC vs. p25 $\alpha$ +vehicle; pS129 aSyn,  $F_{2,21} = 16.61$ ,  $p < 0.001$  LFC vs. p25 $\alpha$ +vehicle,  $p < 0.05$  LFC vs. p25 $\alpha$ +KYP-2047, 1-way ANOVA with Tukey's post hoc test). 48 h treatment with 10  $\mu$ M KYP-2047 significantly decreased both total and pS129 aSyn compared to vehicle

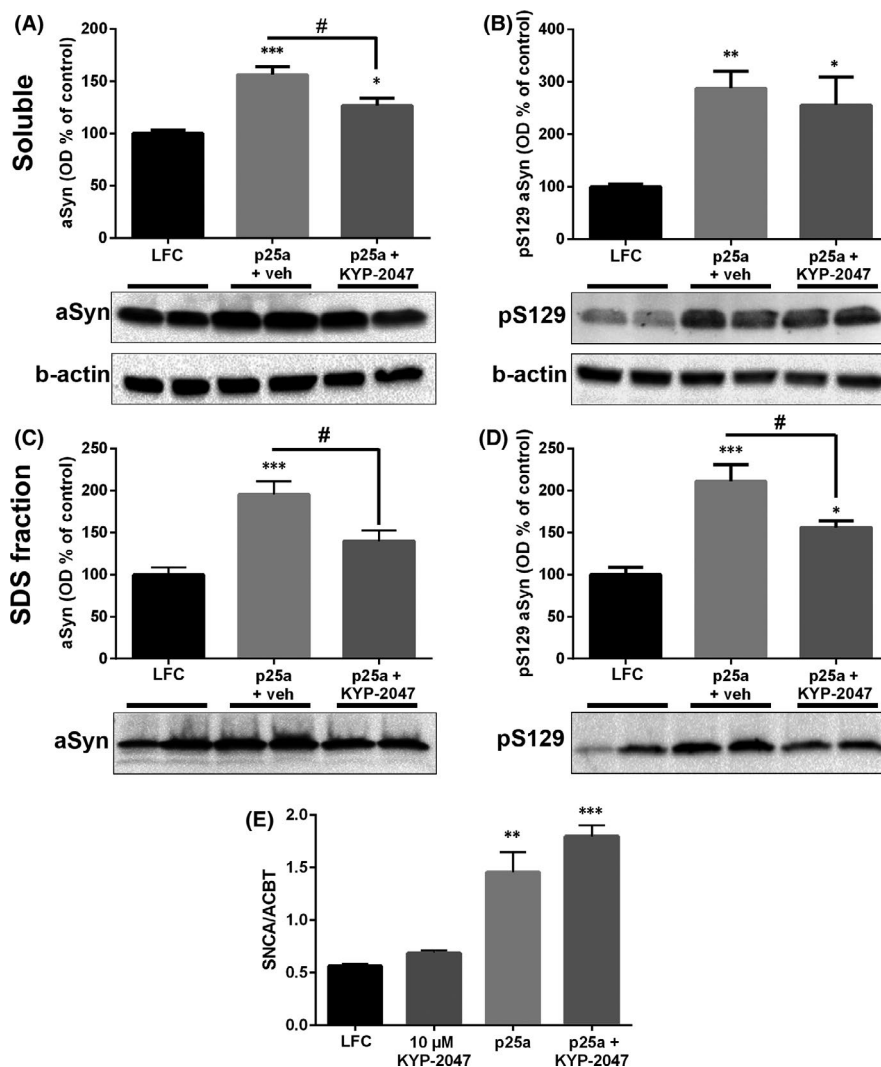


**FIGURE 3** KYP-2047 treatment reduces the levels of aSyn and phosphorylated aSyn in p25 $\alpha$  transfected OLN-AS7 cells. p25 $\alpha$  transfection (p25 $\alpha$ +veh; 0.01% DMSO as vehicle) increased the levels of total aSyn and Ser129 phosphorylated aSyn (pS129) in the soluble fraction (A-B). 48 h treatment with 10  $\mu$ M KYP-2047 (p25 $\alpha$ +KYP-2047) significantly reduced total aSyn levels compared to vehicle treatment (p25 $\alpha$ +veh) (A) but did not have an effect on soluble pS129 aSyn (B). In the SDS fraction, SDS-soluble (monomeric) aSyn and pS129 aSyn were elevated after p25 $\alpha$  transfection but 48 h treatment with KYP-2047 significantly decreased the levels for both proteins (C-D). p25 $\alpha$  transfection elevated significantly the levels of aSyn mRNA (*Snca*) when correlated with the housekeeping gene  $\beta$ -actin (*Acbt*; E). p25 $\alpha$  transfection combined with 48 h KYP-2047 treatment elevated *Snca* levels as well but this was not seen in protein levels (E). Data are presented as mean  $\pm$  SEM. \*,  $p < 0.05$ ; \*\*,  $p < 0.01$ ; \*\*\*,  $p < 0.001$ , 1-way ANOVA with Tukey's post hoc test (compared to vehicle). #,  $p < 0.05$ ; 1-way ANOVA with Tukey's post hoc test (p25 $\alpha$ +veh vs. p25 $\alpha$ +KYP-2047). See figure S4 for uncut blots and for total protein loading control for insoluble fraction

treatment (Figure 3C-D;  $p < 0.05$ , 1-way ANOVA with Tukey's post hoc test). Although clear aSyn and pS129 aSyn signal were detected in the SDS fraction, pointing to aggregation and formation of non-soluble aSyn forms, mostly monomeric aSyn was seen in the SDS fraction (Figure 3A-D; see full membranes and total protein for insoluble fraction in Figure S4). The ratios between pS129 aSyn and aSyn remained unchanged in soluble and SDS fraction but the ratio between insoluble/soluble pS129 aSyn was significantly increased in p25 $\alpha$ +vehicle group (Figure S2;  $F_{2,17} = 6.784$ ,  $p < 0.05$  LFC vs. p25 $\alpha$ +vehicle, 1-way ANOVA with Tukey's post hoc test).

Since the levels of aSyn were significantly elevated after p25 $\alpha$  transfection, we measured if mRNA levels of aSyn (*Snca*) had changed. Interestingly, p25 $\alpha$  transfection alone increased the levels of *Snca* mRNA (Figure 3E;  $F_{3,8} = 28.59$ ,  $p < 0.001$  NC vs. p25 $\alpha$ ;  $p < 0.0001$  p25 $\alpha$  vs. p25 $\alpha$ +KYP-2047; 1-way ANOVA with Tukey's post-test) that explains changes in protein levels and also different staining pattern in ICC (Figure 2). KYP-2047 did not have effect on *Snca* mRNA levels, similar to an earlier study,<sup>26</sup> and KYP-2047 did not alter p25 $\alpha$  levels in OLN-AS7 cells (Figure S3).



### 3.3 | PREP inhibition induces autophagy and re-activates protein phosphatase 2A (PP2A) in OLN-AS7 cells

Our previous results show that PREP inhibition can activate autophagy to reduce aSyn aggregates,<sup>16,17,27</sup> and we recently showed that PREP inhibition induces autophagy by activating PP2A.<sup>25</sup> We studied the levels of the total catalytic subunit of PP2A (PP2Ac) and inactive Tyr307 phosphorylated PP2Ac (pPP2A; antibody specific for inactive PP2A verified in<sup>25</sup>) by WB after p25 $\alpha$  transfection and 48 h treatment by vehicle or KYP-2047. This revealed that p25 $\alpha$  transfection significantly elevated the levels of pPP2A (Figure 4B;  $F_{2,15} = 6.619$ ,  $p < 0.01$  LFC vs. p25 $\alpha$ +vehicle, 1-way ANOVA with Tukey's post hoc test), indicating PP2A inactivation, while treatment with 10  $\mu$ M KYP-2047 restored pPP2A levels close to control level (Figure 4B;  $F_{2,15} = 6.619$ ,  $p < 0.01$  p25 $\alpha$ +vehicle vs. p25 $\alpha$ +KYP-2047, 1-way ANOVA with Tukey's post hoc test).

When we detected the autophagy markers—protein accumulation marker p62 and autophagosome marker LC3BII—in OLN-AS7 cells after p25 $\alpha$  transfection, LC3BII was significantly elevated both in vehicle and KYP-2047 treated cells (Figure 4D; LC3BII;  $F_{2,20} = 12.80$ ,  $p < 0.001$  LFC vs. p25 $\alpha$ +vehicle;  $p < 0.01$  LFC vs. p25 $\alpha$ +KYP-2047, 1-way ANOVA with Tukey's post hoc test). p62 was elevated in p25 $\alpha$ +vehicle group but this was not significant (Figure 4C). However, 10  $\mu$ M KYP-2047 significantly decreased the p62 levels compared to vehicle-treated cells (Figure 4C;  $F_{2,20} = 5.464$ ,  $p < 0.05$  p25 $\alpha$ +vehicle vs. p25 $\alpha$ +KYP-2047, 1-way ANOVA with Tukey's post hoc test). Since p62 was not decreased in p25 $\alpha$ +vehicle group and LC3BII levels were also increased, this suggests decreased degradation of autophagosomes and reduced autophagic flux.<sup>28</sup> In line with decreased aSyn levels in the SDS fraction, 48 h KYP-2047 incubation decreased the levels of p62 that in combination with elevated LC3BII levels indicates increased autophagic flux (Figure 4C-D; both detected from soluble fraction). This also explains why KYP-2047 decreased aSyn levels in ICC and WB although the mRNA expression was not changed.

### 3.4 | p25 $\alpha$ enhances aSyn accumulation and PP2Ac phosphorylation in human oligodendrocyte cells

We wanted to verify the main results seen in OLN-AS7 cells with human oligodendrocyte cell line MO3.13. Cells were transfected with p25 $\alpha$  or aSyn +/- p25 $\alpha$ , and treated with 10  $\mu$ M KYP-2047 for 48 h. Co-transfection of p25 $\alpha$  and aSyn caused significant increase in soluble aSyn compared to empty plasmid (Figure 5A;  $F_{5,12} = 8.842$ ,  $p < 0.05$  empty vs. p25 $\alpha$ +vehicle;  $p < 0.01$  empty vs. p25 $\alpha$ +KYP-2047, 1-way ANOVA with Tukey's post hoc test). Similar to aSyn, pS129 aSyn was also significantly elevated compared to empty transfection (Figure 5B;  $F_{5,12} = 20.98$ ,  $p < 0.001$  empty vs. p25 $\alpha$ +vehicle;  $p < 0.001$  empty vs. p25 $\alpha$ +KYP-2047, 1-way ANOVA with Tukey's post hoc test) but combination of p25 $\alpha$  and aSyn also significantly elevated the levels of pS129 aSyn compared

to aSyn alone (Figure 5B;  $F_{5,12} = 20.98$ ,  $p < 0.001$  aSyn+empty vs. p25 $\alpha$ +vehicle;  $p < 0.001$  aSyn+empty vs. p25 $\alpha$ +KYP-2047, 1-way ANOVA with Tukey's post hoc). Changes in aSyn levels can be explained by positive impact of p25 $\alpha$  on aSyn mRNA expression similar to OLN-AS7 cells (Figure 5E;  $F_{4,12} = 1.286$ ,  $p < 0.001$  p25 $\alpha$ +vehicle vs. p25 $\alpha$ +aSyn and p25 $\alpha$ +aSyn+KYP-2047, 1-way ANOVA with Tukey's post hoc) but significant increase in pS129 aSyn by p25 $\alpha$  co-transfection points to p25 $\alpha$  catalysed aSyn phosphorylation. In the insoluble fraction, p25 $\alpha$  elevated similarly insoluble aSyn but this was not statistically different from aSyn alone (Figure 5C;  $F_{5,12} = 5.481$ ,  $p < 0.05$  empty vs. p25 $\alpha$ +vehicle). However, also insoluble pS129 aSyn was significantly elevated compared to aSyn alone (Figure 5D;  $F_{5,12} = 9.115$ ,  $p < 0.01$  empty vs. p25 $\alpha$ +vehicle,  $p < 0.05$  empty vs. p25 $\alpha$ +KYP-2047;  $p < 0.05$  aSyn+empty vs. p25 $\alpha$ +vehicle and p25 $\alpha$ +KYP-2047, 1-way ANOVA with Tukey's post hoc). However, 10  $\mu$ M KYP-2047 had no impact on any aSyn forms in MO3.13 cells (Figure 5A-D). Additionally, aSyn or aSyn and p25 $\alpha$  co-transfection had no effect on MO3.13 cell viability (Figure 5F).

We further characterized the levels of PP2Ac, pPP2Ac and autophagy markers LC3B and p62 from soluble fractions of MO3.13 cells. Similar to OLN-AS7 cells, total levels of PP2Ac were not altered (Figure 6A) but p25 $\alpha$  transfection alone significantly elevated pPP2Ac levels (Figure 6B;  $F_{5,18} = 4.700$ ,  $p < 0.05$  empty vs. p25 $\alpha$ +empty, 1-way ANOVA with Tukey's post-test). Interestingly, co-transfection of p25 $\alpha$  and aSyn did not have significant effect on pPP2Ac and although KYP-2047 decreased the inactive form of PP2Ac, this was not significant (Figure 6B). Unlike in OLN-AS7 cells, autophagy markers were not altered by p25 $\alpha$  and aSyn (Figure 6C-D).

## 4 | DISCUSSION

MSA is a devastating neurodegenerative disease that lacks disease-modifying therapy. In this study, we have shown that KYP-2047, a PREP inhibitor that has shown beneficial effects in several aSyn-based PD models, protects cells from aSyn toxicity in a cellular model of MSA. Our results demonstrate that in OLN-AS7 cells, KYP-2047 induces autophagy by re-activating PP2A and this leads to decreased levels of aSyn aggregates and elevated cell viability.

Alterations in PREP activity have been reported in several neurodegenerative diseases, including Parkinson's and Alzheimer's diseases,<sup>29,30</sup> but there are no reports about PREP in MSA. PREP activity has been reported in rat oligodendrocytes,<sup>31</sup> but the activity was lower than in neurons or astrocytes. However, in the current study, the PREP activity measured from OLN-AS7 cells was remarkably high when compared, for example to SH-SY5Y neuronal cell culture<sup>26</sup> and p25 $\alpha$  transfection elevated PREP activity. It has been shown that PREP activity and levels are increased in astrocytes and microglial cells when they are activated, suggesting that PREP is inducible in glial cell activation.<sup>29,32</sup> Therefore, it could be possible that PREP is also induced in MSA after p25 $\alpha$  translocation but this requires further studies by using MSA patient material.

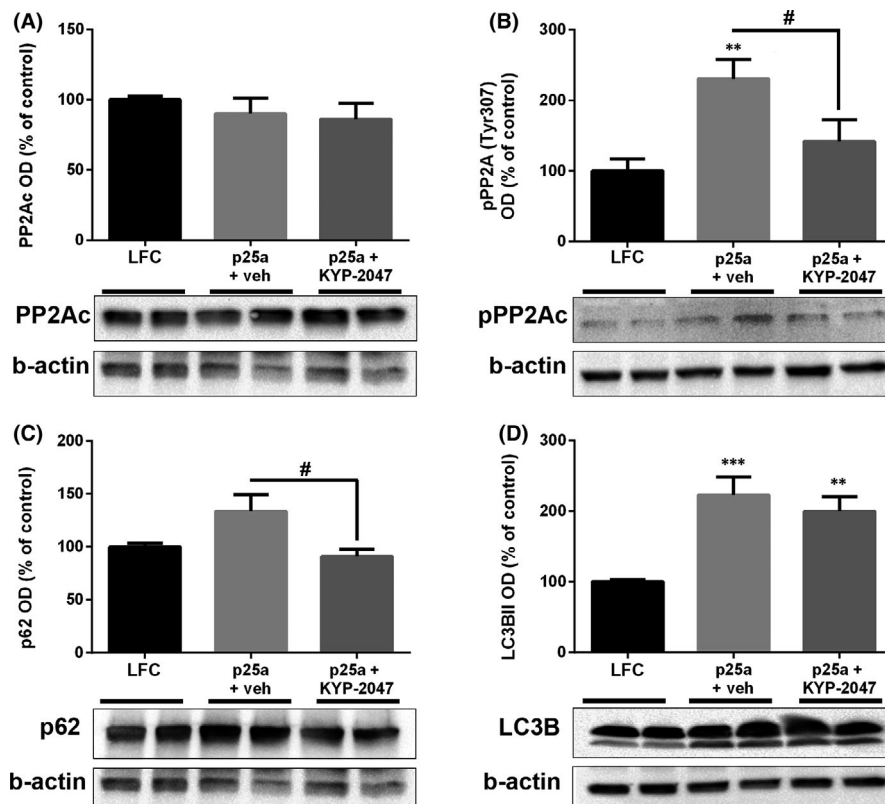


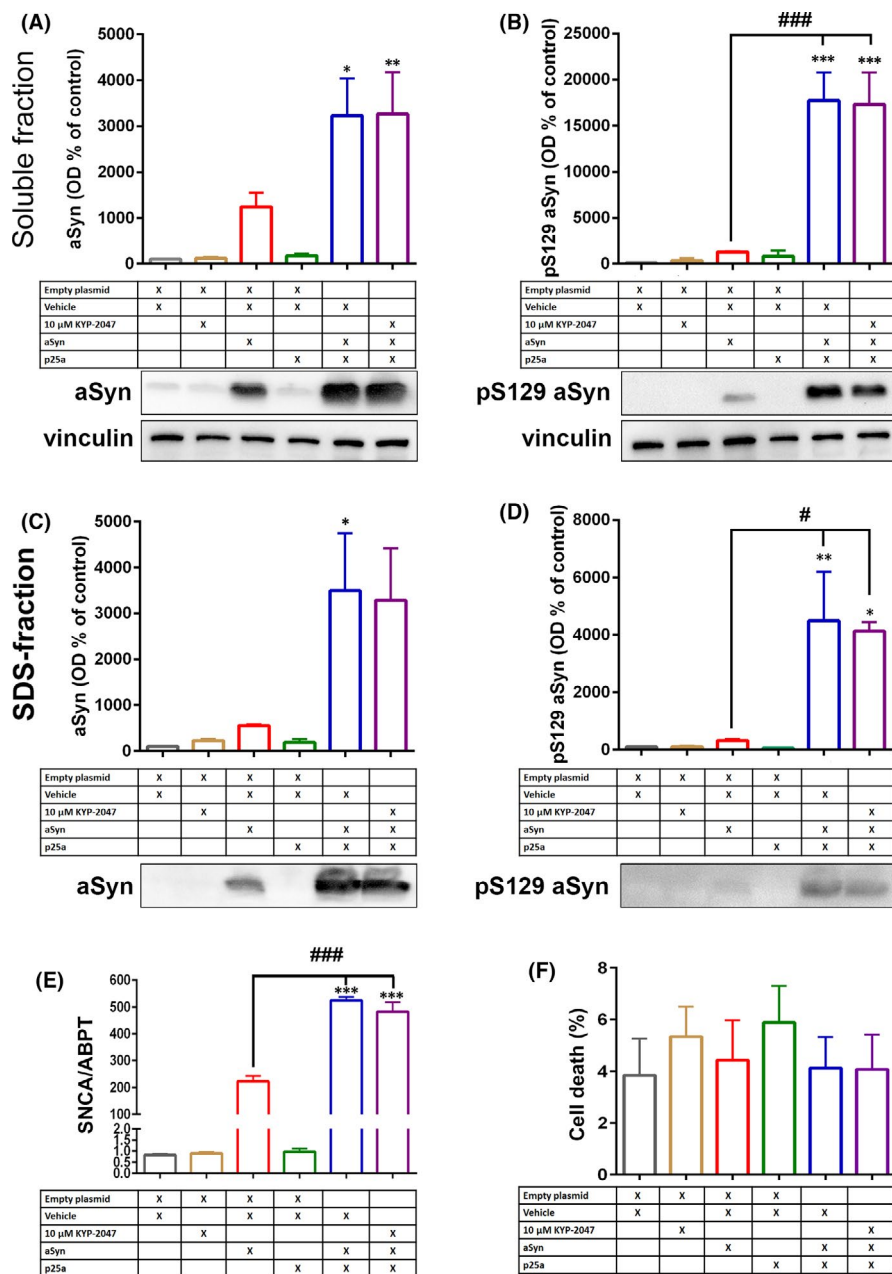
**FIGURE 4** PREP inhibition reduces PP2A phosphorylation and activates autophagy in p25 $\alpha$  transfected OLN-AS7 cells. p25 $\alpha$  transfection did not alter the levels of catalytic subunit of PP2A (A; PP2Ac) but Tyr307 phosphorylated PP2Ac (B; pPP2Ac) was significantly elevated after transfection and vehicle treatment (B). 10  $\mu$ M KYP-2047 significantly reduced pPP2Ac levels compared to p25 $\alpha$ +vehicle but did not change the levels of PP2Ac (A-B). The protein accumulation marker, p62, was significantly decreased in p25 $\alpha$  transfected and KYP-2047 treated cells compared to vehicle treatment (C). Autophagosome marker LC3BII was elevated in p25 $\alpha$  transfected cells and remained elevated after 10  $\mu$ M KYP-2047 treatment (D). Data are presented as mean  $\pm$  SEM. \*,  $p < 0.05$ ; \*\*,  $p < 0.01$ ; \*\*\*,  $p < 0.001$ , 1-way ANOVA with Tukey's post hoc test (compared to vehicle). #,  $p < 0.05$ ; 1-way ANOVA with Tukey's post hoc test (p25 $\alpha$ +veh vs. p25 $\alpha$ +KYP-2047). See figure S5 for uncut blots. Representative blots in Figure 4A and C are from the same membrane and therefore share the beta-actin loading control

Our results revealed that p25 $\alpha$  transfection in OLN-AS7 cells caused increased phosphorylation of PP2A at Tyr307 that is indicative for PP2A inactivation.<sup>33</sup> Interestingly, our recent study showed that PREP negatively regulates PP2A phosphatase functions via protein-protein interactions.<sup>25</sup> Elevated PREP activity after p25 $\alpha$  transfection could contribute to reduced PP2A levels but we cannot exclude the impact of p25 $\alpha$  itself. Lowered PP2A activity has been connected particularly to Alzheimer's disease and tauopathies since PP2A is the most important dephosphorylating phosphatase for Tau.<sup>34</sup> Decreased PP2A levels and activity have been measured in synucleinopathies as well,<sup>35,36</sup> and PP2A can dephosphorylate aSyn at Ser129 thus stabilizing it (see below).<sup>37</sup> Elevated aSyn levels are shown to increase PP2A activity *in vitro*<sup>38</sup> but aggregated aSyn decreases PP2A activity.<sup>39</sup> PP2A regulates, for example autophagy (see below), glutamate receptor recycling and protein stability via dephosphorylation, and decreased PP2A activity can result in several forms of cellular damage in neurodegenerative diseases.<sup>40,41</sup> There are no reports about PP2A levels in MSA, or a connection between p25 $\alpha$  and PP2A, but our finding

suggests that this should be further studied and that PP2A inactivation could contribute to MSA as well.

p25 $\alpha$  transfection in both cell lines elevated the levels of aSyn and pS129 aSyn both in soluble and insoluble fractions that may well cause cellular toxicity.<sup>10,23</sup> Interestingly, p25 $\alpha$  transfection also increased the levels of aSyn mRNA in both cell lines, suggesting that translocation of p25 $\alpha$  could induce aSyn expression and this way elevate aSyn levels in oligodendrocytes. However, aSyn mRNA has not been reported to be significantly elevated in oligodendrocytes of MSA patients,<sup>9</sup> and our finding requires further verification. Our data shows that KYP-2047 treatment reduced the levels of insoluble pS129 aSyn but had no effect on the levels of soluble pS129 aSyn in OLN-AS7 cells. However, similar impact by KYP-2047 was not seen in MO3.13 cells. This could be due the enormous aSyn overexpression that is significantly higher than, for example in stably aSyn overexpressing SH-SY5Y cells where PREP inhibitors have shown good effects.<sup>26</sup> Additionally, the aSyn plasmid used in the study has a V5-tag in its C-terminus.<sup>17</sup> The results by Savolainen et al. (2015)<sup>15</sup> showed that truncation of C-terminus disturbs the

**FIGURE 5** p25 $\alpha$  transfection elevates aSyn levels and phosphorylation in MO3.13 cells. p25 $\alpha$  co-transfection with aSyn elevated aSyn levels both in soluble and SDS fraction (A, C). After 48h co-transfection, pS129 aSyn was increased significantly compared to empty control and aSyn+empty in both fractions (B, D). This was in correlation with mRNA levels where similar increase in aSyn mRNA expression was seen when co-transfected with p25 $\alpha$  (E; SNCA). However, no changes in cell viability were seen by any transfections or treatments (F), and 10  $\mu$ M KYP-2047 had no effect on aSyn levels or aSyn mRNA. Data are presented as mean  $\pm$  SEM.  $p < 0.05$ ; \*\*,  $p < 0.01$ ; \*\*\*,  $p < 0.001$ , 1-way ANOVA with Tukey's post hoc test (compared to empty plasmid). #,  $p < 0.05$ ; ###,  $p < 0.001$  1-way ANOVA with Tukey's post hoc test (aSyn+empty+veh vs. p25 $\alpha$ +aSyn+veh or p25 $\alpha$ +aSyn+KYP-2047). See figure S6 for uncut blots and for total protein loading control for insoluble fraction. Representative blots in Figures 5A and 6C are from the same membrane and therefore share the vinculin loading control



interaction between PREP and aSyn, and it is possible that tagged aSyn is not optimal for PREP interaction, and therefore, the impact of PREP inhibitor is also altered. This view is supported also by an earlier study by Svarebans et al. (2018),<sup>16</sup> where the same plasmid was used but the deletion of PREP did not have significant effect on aSyn levels although PREP deleted HEK-293 cells had significantly accelerated autophagic flux.

Phosphorylation of aSyn has been under intensive studies since normally only a small portion of brain aSyn is phosphorylated but in synucleinopathies the ratio of pS129 aSyn increases substantially.<sup>5</sup> However, it is still under debate how this post-translational modification is related to synucleinopathies and aSyn toxicity. aSyn phosphorylation at serine 129 may change its membrane binding and interaction partners, and it also increased nuclear localization of aSyn that may interfere with gene functions<sup>42</sup> but toxicity of pS129

aSyn *in vivo* has remained controversial (for review, see<sup>43</sup>). On the other hand, aSyn phosphorylation at serine 129 increases its turnover in cells, and it has been suggested that Ser129 phosphorylation targets aSyn for proteasomal degradation.<sup>44</sup> Therefore, it is possible that when KYP-2047 induced autophagy, this reduced proteasomal activity in the cells (for review about the interplay between proteasomal and autophagy systems, see<sup>45</sup>) as we have reported in PREP knock-out HEK-293 cells,<sup>16</sup> and caused the increase in soluble pS129 aSyn.

Monomeric aSyn is degraded via proteasomes and chaperone-mediated autophagy but these systems are easily damaged by aSyn aggregates, leading to elevated aSyn concentrations and aggregation.<sup>46,47</sup> Macroautophagy (autophagy) is able to degrade aSyn oligomers and larger aggregates,<sup>48</sup> and the activation of autophagy has been suggested as a possible therapy against synucleinopathies and

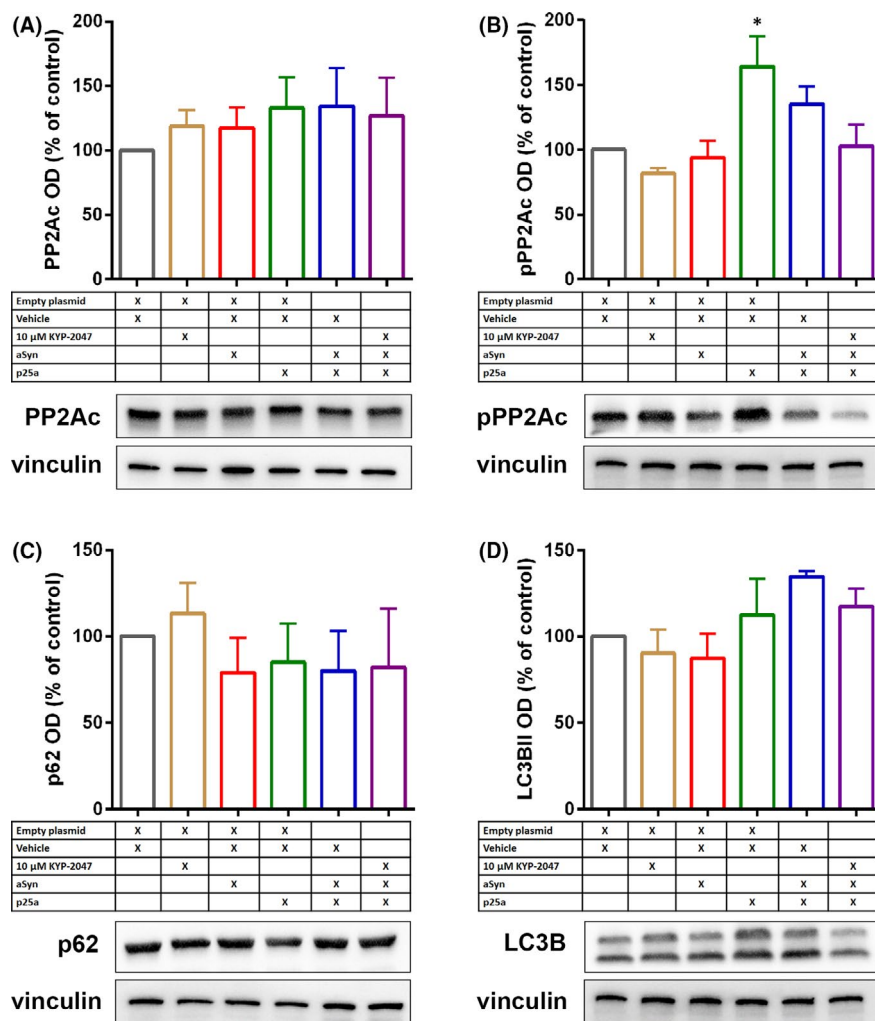


**FIGURE 6** p25 $\alpha$  transfection increases PP2A phosphorylation in MO3.13 cells. Similar to OLN-AS7 cells, p25 $\alpha$ , aSyn or p25 $\alpha$ +aSyn transfection did not alter the levels of catalytic subunit of PP2A (A; PP2Ac). However, Tyr307 phosphorylated PP2Ac (B; pPP2Ac) was significantly increased by p25 $\alpha$  transfection but not with other combinations. 10  $\mu$ M KYP-2047 reduced pPP2Ac levels but not significantly (B). p62 or autophagosome marker LC3BII were not altered by p25 $\alpha$ , aSyn or their combination in MO3.13 cells (C-D). Data are presented as mean  $\pm$  SEM. \*,  $p < 0.05$ ; empty+veh vs. p25 $\alpha$ +veh, 1-way ANOVA with Tukey's post hoc test. See figure S7 for uncut blots. Representative blots in Figure 6B and D are from the same membrane and therefore share the vinculin loading control

other neurodegenerative diseases (for reviews, see<sup>6,49</sup>). Impaired autophagy has been reported in MSA patient samples and patient-derived induced pluripotent stem cells,<sup>50,51</sup> and it may well contribute to oligodendroglial aSyn accumulation and toxicity. We also showed here that in OLN-AS7 cells, p25 $\alpha$  transfection caused intracellular accumulation of autophagosomes and aggregation markers, indicating reduced autophagic flux. This is in line with a previous study, where p25 $\alpha$  and aSyn together interfered with autophagosome-lysosome interaction, and p25 $\alpha$  alone impaired autophagosome formation.<sup>52</sup> Although aSyn and p25 $\alpha$  co-transfection significantly elevated aSyn phosphorylation both in soluble and insoluble fractions, this did not cause any changes in autophagy markers in MO3.13 cells. aSyn and p25 $\alpha$  overexpression also did not have effect on cell viability of MO3.13 cells, and this emphasizes the importance of normal autophagy for cellular toxicity of aSyn. It is possible that p25 $\alpha$ -induced PP2A inactivation is behind reduced autophagosome formation since PP2A regulates autophagy via mTOR and beclin1 pathways that are responsible for autophagy initiation and autophagosome formation, respectively.<sup>53,54</sup> Autophagy activators attenuated symptoms in a mouse model of MSA,<sup>14,55</sup> and our results with KYP-2047 indicate that autophagy activation reduces p25 $\alpha$  transfection induced aSyn toxicity in OLN-AS7 cells by removing particularly insoluble aSyn species.

Taken together, our data suggest that p25 $\alpha$  transfection to cellular models of MSA induces not only aSyn phosphorylation and aggregation but also PP2A inactivation. Additionally, our results suggest that autophagy impairment is important step for aSyn-induced toxicity in cellular models of MSA. In OLN-AS7 cells, PREP inhibition after p25 $\alpha$  transfection re-activated PP2A, reduced both total and pSer129 aSyn in the insoluble fraction by inducing autophagy and attenuated the toxicity of aSyn in in OLN-AS7 cellular model of MSA. Our results suggest that PREP inhibition could be a possible disease-modifying therapy that is applicable for several synucleinopathies.

#### ACKNOWLEDGEMENTS

The work was supported by grants from Academy of Finland (grant 318327), Jane and Aatos Erkkö Foundation and Sigrid Juselius Foundation grants for TTM. PHJ was supported by the Lundbeck Foundation with grants R248-2016-2518 (Danish Research Institute of Translational Neuroscience–DANDRITE, Nordic-EMBL Partnership for Molecular Medicine) and R223-2015-4222 (Decisive and early alpha-synuclein aggregate dependent calcium changes in Parkinson's disease).

#### CONFLICTS OF INTEREST

The authors confirm that there are no conflicts of interest.

## AUTHOR CONTRIBUTIONS

**Hengjing Cui:** Formal analysis (equal); Investigation (equal); Methodology (equal); Validation (equal); Writing-original draft (equal). **Tommi Kilpeläinen:** Conceptualization (equal); Formal analysis (equal); Funding acquisition (equal); Investigation (equal); Writing-original draft (equal). **Lydia Zouzoula:** Investigation (equal); Methodology (equal); Writing-original draft (equal). **Samuli Auno:** Conceptualization (equal); Formal analysis (equal); Funding acquisition (equal); Investigation (equal); Writing-original draft (equal). **Kalevi Trontti:** Investigation (supporting); Methodology (supporting); Writing-review & editing (supporting). **Sampo Kurvonen:** Investigation (supporting); Methodology (supporting); Writing-review & editing (supporting). **Susanna Norrbacka:** Formal analysis (supporting); Investigation (supporting); Methodology (supporting). **Iiris Hovatta:** Project administration (supporting); Resources (supporting); Supervision (supporting); Writing-review & editing (supporting). **Poul Henning Jensen:** Resources (supporting); Writing-review & editing (supporting). **Timo T Myöhänen:** Funding acquisition (lead); Project administration (lead); Supervision (lead); Visualization (lead); Writing-review & editing (lead).

## DATA AVAILABILITY STATEMENT

All data generated or analysed during this study are included in this published article. Raw values are available from the corresponding author on reasonable request.

## ORCID

Timo T. Myöhänen  <https://orcid.org/0000-0002-9277-6687>

## REFERENCES

- Gilman S, Wenning GK, Low PA, et al. Second consensus statement on the diagnosis of multiple system atrophy. *Neurology*. 2008;71(9):670-676.
- Papp MI, Kahn JE, Lantos PL. Glial cytoplasmic inclusions in the CNS of patients with multiple system atrophy (striatonigral degeneration, olivopontocerebellar atrophy and Shy-Drager syndrome). *J Neurol Sci*. 1989;94:79-100.
- Wakabayashi K, et al. Accumulation of  $\alpha$ -synuclein/NACP is a cytopathological feature common to Lewy body disease and multiple system atrophy. *Acta Neuropathologica*. 1998;96:445-452.
- Gai WP, et al.  $\alpha$ -Synuclein fibrils constitute the central core of oligodendroglial inclusion filaments in multiple system atrophy. *Exp Neurol*. 2003;181:68-78.
- Fujiwara H, et al.  $\alpha$ -Synuclein is phosphorylated in synucleinopathy lesions. *Nat Cell Biol*. 2002;4:160-164.
- Wong YC, Krainc D. [alpha]-synuclein toxicity in neurodegeneration: mechanism and therapeutic strategies. *Nat Med*. 2017;23:1-13.
- Kahle PJ, et al. Hyperphosphorylation and insolubility of alpha-synuclein in transgenic mouse oligodendrocytes. *EMBO Rep*. 2002;3:583-588.
- Shults CW, et al. Neurological and neurodegenerative alterations in a transgenic mouse model expressing human alpha-synuclein under oligodendrocyte promoter: implications for multiple system atrophy. *J Neurosci*. 2005;25:10689-10699.
- Asi YT, Simpson JE, Heath PR, et al. Alpha-synuclein mRNA expression in oligodendrocytes in MSA. *Glia*. 2014;62:964-970.
- Mavroei P, Arvanitaki F, Karakitsou A-K, et al. Endogenous oligodendroglial alpha-synuclein and TPPP/p25 $\alpha$  orchestrate alpha-synuclein pathology in experimental multiple system atrophy models. *Acta Neuropathologica*. 2019;138:415-441.
- Tirián L, Hlavanda E, Olah J, et al. TPPP/p25 promotes tubulin assemblies and blocks mitotic spindle formation. *Proc Natl Acad Sci USA*. 2003;100:13976-13981.
- Ota K, Obayashi M, Ozaki K, et al. Relocation of p25 $\alpha$ /tubulin polymerization promoting protein from the nucleus to the perinuclear cytoplasm in the oligodendroglia of sporadic and COQ2 mutant multiple system atrophy. *Acta Neuropathologica Communications*. 2014;2:136.
- Heras-Garvin A, Weckbecker D, Ryazanov S, et al. Anle138b modulates  $\alpha$ -synuclein oligomerization and prevents motor decline and neurodegeneration in a mouse model of multiple system atrophy. *Movement Disord*. 2019;34:255-263.
- Pukaß K, Richter-Landsberg C. Inhibition of UCH-L1 in oligodendroglial cells results in microtubule stabilization and prevents  $\alpha$ -synuclein aggregate formation by activating the autophagic pathway: implications for multiple system atrophy. *Front Cell Neurosci*. 2015;9:163.
- Savolainen MH, Yan X, Myöhänen TT, Huttunen HJ. Prolyl Oligopeptidase enhances  $\alpha$ -synuclein dimerization via direct protein-protein interaction. *J Biol Chem*. 2015;290:5117-5126.
- Svarcbahs R, Julku UH, Norrbacka S, Myöhänen TT. Removal of prolyl oligopeptidase reduces alpha-synuclein toxicity in cells and in vivo. *Sci Rep*. 2018;8:1552.
- Savolainen MH, et al. The beneficial effect of a prolyl oligopeptidase inhibitor, KYP-2047, on alpha-synuclein clearance and autophagy in A30P transgenic mouse. *Neurobiol Dis*. 2014;68:1-15.
- Kilpeläinen TP, Hellinen L, Vrijdag J, et al. The effect of prolyl oligopeptidase inhibitors on alpha-synuclein aggregation and autophagy cannot be predicted by their inhibitory efficacy. *Biomed Pharmacother*. 2020;128:110253.
- Kilpeläinen TP, Tyni JK, Lahtela-Kakkonen MK, et al. Tetrazole as a replacement of the electrophilic group in characteristic prolyl oligopeptidase inhibitors. *ACS Med Chem Lett*. 2019;10(12):1635-1640.
- Rostami J, et al. Prolyl oligopeptidase inhibition by KYP-2407 increases alpha-synuclein fibril degradation in neuron-like cells. *Biomed Pharmacother*. 2020;131:110788.
- Svarcbahs R, Julku UH, Myöhänen TT. Inhibition of prolyl oligopeptidase restores spontaneous motor behavior in the  $\alpha$ -synuclein virus vector-based Parkinson's disease mouse model by decreasing  $\alpha$ -synuclein oligomeric species in mouse brain. *J Neurosci*. 2016;36:12485-12497.
- Jarho EM, et al. A cyclopent-2-enecarbonyl group mimics proline at the P2 position of prolyl oligopeptidase inhibitors. *J Med Chem*. 2004;47:5605-5607.
- Kragh CL, et al. Alpha-synuclein aggregation and Ser-129 phosphorylation-dependent cell death in oligodendroglial cells. *J Biol Chem*. 2009;284:10211-10222.
- Lindersson E, Lundvig D, Petersen C, et al. p25 $\alpha$  stimulates  $\alpha$ -synuclein aggregation and is co-localized with aggregated  $\alpha$ -synuclein in  $\alpha$ -synucleinopathies. *J Biol Chem*. 2005;280:5703-5715.
- Svarcbahs R, Jääntti M, Kilpeläinen T, et al. Prolyl oligopeptidase inhibition activates autophagy via protein phosphatase 2A. *Pharmacol Res*. 2020;151:104558.
- Myöhänen TT, et al. A prolyl oligopeptidase inhibitor, KYP-2047, reduces alpha-synuclein protein levels and aggregates in cellular and animal models of Parkinson's disease. *Br J Pharmacol*. 2012;166:1097-1113.
- Myöhänen TT, Norrbacka S, Savolainen MH. Prolyl oligopeptidase inhibition attenuates the toxicity of a proteasomal inhibitor, lactacystin, in the alpha-synuclein overexpressing cell culture. *Neurosci Lett*. 2017;636:83-89.

28. Klionsky DJ, et al. Guidelines for the use and interpretation of assays for monitoring autophagy (3rd edition). *Autophagy* 2016;12:1-222.
29. Hannula MJ, Myohanen TT, Tenorio-Laranga J, Mannisto PT, Garcia-Horsman JA. Prolyl oligopeptidase colocalizes with alpha-synuclein, beta-amyloid, tau protein and astroglia in the post-mortem brain samples with Parkinson's and Alzheimer's diseases. *Neurosci*. 2013;242:140-150.
30. Aoyagi T, Wada T, Nagai M, et al. Deficiency of kallikrein-like enzyme activities in cerebral tissue of patients with Alzheimer's disease. *Experientia*. 1990;46:94-97.
31. Mentlein R, von Kolszynski M, Sprang R, Lucius R. Proline-specific proteases in cultivated neuronal and glial cells. *Brain Res*. 1990;527:159-162.
32. Natunen TA, Gynther M, Rostalski H, Jaako K, Jalkanen AJ. Extracellular prolyl oligopeptidase derived from activated microglia is a potential neuroprotection target. *Basic Clin Pharmacol Toxicol*. 2019;124:40-49.
33. Chen J, Martin B, Brautigan D. Regulation of protein serine-threonine phosphatase type-2A by tyrosine phosphorylation. *Science*. 1992;257:1261-1264.
34. Sontag J-M, Sontag E. Protein phosphatase 2A dysfunction in Alzheimer's disease. *Front Mol Neurosci*. 2014;7. <https://doi.org/10.3389/fnmol.2014.00016>
35. Park H-J, Lee K-W, Park ES, et al. Dysregulation of protein phosphatase 2A in parkinson disease and dementia with lewy bodies. *Ann Clin Transl Neurol*. 2016;3:769-780.
36. Yang W, Li X, Yin N.  $\alpha$ -Syn oligomers incubated with Parkinson's disease plasma promote neuron damage. *Int J Clin Exp Pathol*. 2020;13:1995-2008.
37. Pérez-Revuelta BI, et al. Metformin lowers Ser-129 phosphorylated  $\alpha$ -synuclein levels via mTOR-dependent protein phosphatase 2A activation. *Cell Death Dis*. 2014;5:e1209.
38. Qu J, et al. The Molecular mechanism of alpha-synuclein dependent regulation of protein phosphatase 2A activity. *Cell Physiol Biochem*. 2018;47:2613-2625.
39. Wu J, Lou H, Alerte T, et al. Lewy-like aggregation of  $\alpha$ -synuclein reduces protein phosphatase 2A activity in vitro and in vivo. *Neuroscience*. 2012;207:288-297.
40. O'Connor CM, Perl A, Leonard D, Sangodkar J, Narla G. Therapeutic targeting of PP2A. *Int J Biochem Cell Biol*. 2017;96:182-193.
41. Zimmer ER, Leuzy A, Souza DO, Portela LV. Inhibition of Protein Phosphatase 2A: focus on the glutamatergic system. *Mol Neurobiol*. 2016;53:3753-3755.
42. Pinho R, et al. Nuclear localization and phosphorylation modulate pathological effects of alpha-synuclein. *Hum Mol Genet*. 2018;28:31-50.
43. Oueslati A. Implication of alpha-synuclein phosphorylation at s129 in synucleinopathies: what have we learned in the last decade? *J Parkinson's Dis*. 2016;6:39-51.
44. Machiya Y, et al. Phosphorylated alpha-synuclein at Ser-129 is targeted to the proteasome pathway in a ubiquitin-independent manner. *J Biol Chem*. 2010;285:40732-40744.
45. Kocaturk Nur Mehpare, Gozuacik Devrim. Crosstalk between mammalian autophagy and the ubiquitin-proteasome system. *Front Cell Dev Biol*. 2018;6:128.
46. Cuervo AM, Stefanis L, Fredenburg R, Lansbury PT, Sulzer D. Impaired degradation of mutant alpha-synuclein by chaperone-mediated autophagy. *Science*. 2004;305:1292-1295.
47. Ebrahimi-Fakhari D, et al. Distinct roles in vivo for the ubiquitin-proteasome system and the autophagy-lysosomal pathway in the degradation of alpha-synuclein. *J Neurosci*. 2011;31:14508-14520.
48. Gao J, Perera G, Bhadbhade M, Halliday GM, Dzamko N. Autophagy activation promotes clearance of  $\alpha$ -synuclein inclusions in fibril-seeded human neural cells. *J Biol Chem*. 2019;294(39):14241-14256.
49. Menzies FM, et al. Autophagy and neurodegeneration: pathogenic mechanisms and therapeutic opportunities. *Neuron*. 2017;93:1015-1034.
50. Schwarz L, Goldbaum O, Bergmann M. Involvement of macroautophagy in multiple system atrophy and protein aggregate formation in oligodendrocytes. *J Mol Neurosci*. 2012;47:256-266.
51. Monzio Compagnoni G, et al. Mitochondrial dysregulation and impaired autophagy in iPSC-derived dopaminergic neurons of multiple system atrophy. *Stem Cell Rep*. 2018;11:1185-1198.
52. Ejlerskov P, et al. Promotes unconventional secretion of  $\alpha$ -synuclein through exophagy by impairing autophagosome-lysosome fusion. *J Biol Chem*. 2013;288:17313-17335.
53. Yeasmin AMST, Waliullah TM, Kondo A, et al. Orchestrated action of PP2A antagonizes Atg13 phosphorylation and promotes autophagy after the inactivation of TORC1. *PLoS ONE*. 2016;11:e0166636.
54. Fujiwara N, Usui T, Ohama T, Sato K. Regulation of beclin 1 protein phosphorylation and autophagy by protein phosphatase 2A (PP2A) and death-associated protein kinase 3 (DAPK3). *J Biol Chem*. 2016;291:10858-10866.
55. Bai X, et al. Rapamycin improves motor function, reduces 4-hydroxynonenal adducted protein in brain, and attenuates synaptic injury in a mouse model of synucleinopathy. *Pathobiol Aging Age Relat Dis*. 2015;5:28743.

## SUPPORTING INFORMATION

Additional supporting information may be found online in the Supporting Information section.

**How to cite this article:** Cui H, Kilpeläinen T, Zouzoula L, et al. Prolyl oligopeptidase inhibition reduces alpha-synuclein aggregation in a cellular model of multiple system atrophy. *J Cell Mol Med*. 2021;25:9634–9646. <https://doi.org/10.1111/jcmm.16910>